Journal of
Proteomics & Bioinformatics

Liang et al., J Proteomics Bioinform 2013, S7
DOI: 10.4172/jpb.S7-003

Research Article Open Access

Quantitative Proteomics Analysis of Differentially Expressed Proteins Involved in Renal Clear Cell Carcinoma by Shotgun Approach Coupled with Stable Isotope Dimethyl Labeling

Shih-Shin Liang[1,2#], Chao-Jen Kuo[3#], Shu-Wen Chi[3], Wen-Jeng Wu[4], Shui-Tein Chen[5,6] and Shyh-Horng Chiou[3,5*]

[1]*Department of Biotechnology, College of Life Science, Kaohsiung Medical University, Taiwan*
[2]*Center for Research Resources and Development, Kaohsiung Medical University, Taiwan*
[3]*Graduate Institute of Medicine, College of Medicine, Kaohsiung Medical University, Taiwan*
[4]*Department of Urology, Kaohsiung Medical University Hospital, Kaohsiung Medical University, Taiwan*
[5]*Institute of Biological Chemistry, Academia Sinica, Taipei, Taiwan*
[6]*Institute of Biochemical Sciences, College of Life Science, National Taiwan University, Taipei, Taiwan*
[#]*These two authors contribute equally to this study*

Abstract

Renal clear cell carcinoma (RCC) when detected incidentally by ultrasonic imaging generally shows an advanced disease stage of being diagnosed metastatic as a result of lacking specific biomarkers at an early stage. To date, RCC is still ranked as the most common renal cancer and considered as one of the most treatment-resistant metastatic malignancies. In this study, a quantitative proteomics approach by means of gel-free shotgun proteomics methodology and stable isotope dimethyl labeling coupled with nano-liquid chromatography/ tandem mass (nanoLC-MS/MS) have been employed to identify 18 up-regulated and 48 down-regulated proteins in RCC samples. It is worth noting that binding and structural proteins in renal clear cells accounted for 43% and 33% of up-regulated proteins respectively, while catalytic enzymes occupied as high as 73% of down-regulated proteins. Collectively, instead of one universal tumorigenesis enzyme being identified, the pathogenesis of RCC may involve a variety of protein factors including ANXA2, LGALS1, VIM and TPM1 related to metastasis, angiogenesis, tumor invasion as well as tumor growth, in addition to CRYAB, GSTA1, CALB1 and HSPD1, which are linked to apoptosis function. The upshot of this study highlighted by a series of down-regulated proteins suggests that the clear-cut decrease of ATP generation components related to mitochondrial dysfunction and altered energy metabolism may be involved in RCC carcinogenesis.

Keywords: Quantitative proteomics; Renal clear cell carcinoma (RCC); Shotgun proteomics analysis; Nano-liquid chromatography coupled tandem mass spectrometry (nanoLC-MS/MS); Stable isotope dimethyl labeling

Introduction

Renal clear cell carcinoma (RCC), the most frequently occurring form of malignant kidney tumors, originates in the renal cortex, accounting for about 3% of adult malignancies and generally shows no obvious symptom at an early stage [1,2]. To date, RCC is still ranked as the most common renal cancer and considered as one of the most treatment-resistant metastatic malignancies. Epidemiologic studies have demonstrated that taking amphetamine-containing diet pills regularly results in a 2-fold increase in RCC risk, and especially the risk rises along with the increasing dosage of amphetamines [3]. Furthermore, smoking, overweight, hypertension, obesity and dialysis for advanced kidney disease are also established as risk factors for RCC; however, no specific carcinogens have been identified [3-5]. Previous reports based on histopathological studies revealed that RCC, characterized by abnormal deposition with a high concentration of glycogen and lipid [6,7], displayed clinical manifestations and resistance to radiotherapy and chemotherapy. Immunocytochemical studies also suggested that RCC-derived gangliosides significantly suppress nuclear factor-kappa B activation in T cells and indirectly decrease antitumor immune responses in patients with RCCs [8].

Examination and analysis based on the Cleveland Clinic Foundation's nephrectomy database with a 10-year follow-up study demonstrated that the width of the resection margin after nephron-sparing surgery (NSS) for RCC does not significantly correlate with long-term disease progression [9,10]. Namely, tumor size and stage cannot be employed as prognostic factors. In addition, RCC greatly shows a high proportion of metastasis when detected incidentally by ultrasonic imaging in an advanced stage due to the lack of specific biomarkers for early detection [11]. Taken together, historically RCC has been classified as a recalcitrant malignancy for diagnosis and treatment. Therefore, the surgical approach via a radical or partial nephrectomy remains the indispensable practice for the eradication of carcinoma as well as the curative mainstay treatment [12]. Up to now, many clinical research outcomes have not yet offered the potential or optimizing approach for personalizing treatment of individual patients, even though numerous underlying investigations concerning the abnormalities of RCC based on biochemical, cellular and morphological characterizations have been conducted [6,8,13-18].

On the basis of elucidating the cellular dysfunction mediated by some functional proteins within RCC, the recent advent of proteomics methodology have made the reliable and high-throughput identification

***Corresponding author:** Shyh-Horng Chiou, Quantitative Proteomics Center and Graduate Institute of Medicine, Kaohsiung Medical University, Kaohsiung 80708, Taiwan, Tel: +886-7-3220377; Fax: +886-7-3133434; E-mail: shchiou@kmu.edu.tw

Received October 23, 2013; **Accepted** December 23, 2013; **Published** December 26, 2013

Citation: Liang SS, Kuo CJ, Chi SW, Wu WJ, Chen ST, et al. (2013) Quantitative Proteomics Analysis of Differentially Expressed Proteins Involved in Renal Clear Cell Carcinoma by Shotgun Approach Coupled with Stable Isotope Dimethyl Labeling. J Proteomics Bioinform S7: 003. doi:10.4172/jpb.S7-003

of complex protein mixtures in biological tissues less tedious and more amendable to the comprehensive global analysis [19,20]. The study of proteins at the level of the molecular and cellular systems by means of fast-evolving and state-of-the-art proteomics approach has provided a firm basis for unraveling the complex proteome profiles of total protein mixtures from whole tissues or cells of various sources [21]. Therefore, proteomic techniques have been employed to analyze the protein expression profile in elucidating the biochemical development and candidate biomarkers of RCC [20,22-25] with some success. The results suggest that RCC formation is highly correlated with metabolic incoordination and biochemical dysfunctions. However, many differentially expressed proteins or unknown regulatory factors which may play crucial roles in RCC abnormalities have not been identified in the previous studies and remain to be explored.

In this study we aim to conduct the comparative and quantitative proteome analysis between RCC and their nearby normal portion of the same tissue by means of gel-free shotgun proteomic approach coupled with stable isotope dimethyl labeling and nanoLC-MS/MS [26-29]. The differentially expressed proteins identified by the quantitative approach will be employed to delineate the biosignaling pathways involved in the tumorigenesis of RCC. These results may help not only elucidate the pathogenesis of altered cellular function but also identify potential cellular targets for effective therapeutic application.

Materials and Methods

Chemicals and reagents

Quantitative reagent for protein contents was purchased from Bio-Rad (Hercules, CA). Trichloroacetic acid (TCA), trifluoroacetic acid (TFA), dithiothreitol (DTT), iodoacetamide (IAM), ethylenediaminetetraacetic acid (EDTA), sodium deoxycholate, sodium fluoride (NaF), formaldehyde-H_2, formaldehyde-D_2 and ammonium bicarbonate (NH_4HCO_3), Triton X-100 were purchased from Sigma Aldrich (St. Louis, MO). Acetonitrile (ACN) and sodium phosphate were obtained from Merck (Darmstadt, Germany). Formic acid (FA), sodium acetate, sodium cyanoborohydride and sodium chloride (NaCl) were purchased from Riedel-de Haven (Seelze, Germany). Proteinase inhibitors (Complete™ Mini) were purchased from Roche (Mannheim, Germany). Sodium dodecyl sulfate (SDS) and urea were purchased from Amresco (Solon, OH). Modified sequencing-grade trypsin for in-gel digestion was purchased from Promega (Madison, WI). Water was deionized to 18 MΩ by a Milli-Q system (Millipore, Bedford, MA).

Sample collection

All the procedures used in this study were approved by the Ethical Committee of Clinical Research at Kaohsiung Medical University Hospital. We obtained RCC tissues and segmental parts of normal samples adjacent to RCC as controls from five patients who underwent the removal of RCC.

Normal or RCC tissues per gram were homogenized with the aid of a Polytron homogenizer in 1.5 mL extraction buffer (containing 10 mM Tris-HCl pH 7.4, 10 mM sodium phosphate, 150 mM NaCl, 0.1% SDS, 2 mM EDTA, 1% sodium deoxycholate, 100 mM NaF, 1% Triton X-100 and protease-inhibitor cocktail). The homogenates were transferred to 1.5 mL Eppendorf tubes and centrifuged at 13,000xg for 20 min at 4°C to remove debris and insoluble material. Aliquots of the supernatants were assayed for determination of total protein concentration using Coomassie protein assay reagent, and subsequently were stored at -80°C until analyzed.

Dimethyl labeling and peptide preparation

Volumes of lysates containing 100 μg of total proteins from normal or RCC tissues were adjusted to 60 μL and treated with 0.7 μL of 1 M DTT and 9.3 μL of 7.5% SDS at 95°C for 5 min before reduction. After the reaction, lysates were further treated with 8 μL of 50 mM IAM at room temperature for 30 min alkylation in the dark; subsequently proteins were precipitated by adding 52 μL of 50% TCA and incubated on ice for 15 min. After removing the supernatant by centrifugation at 13,000 x g for 5 min, the collected proteins were washed with 150 μL of 10% TCA, vortexed and centrifuged at 13,000 x g for 10 min. The precipitated proteins were washed again with 250 μL distilled H_2O, vortexed and centrifuged under the same condition for 3 times. The resultant pellets were resuspended with 50 mM NH_4HCO_3 (pH 8.5), then digested with 4 μg of trypsin for 8 h at 37°C and further dried in a vacuum centrifuge to remove NH_4HCO_3. The lyophilized peptides for normal and RCC samples re-dissolved in 180 μL of 100 mM sodium acetate at pH 5.5 were treated with 10 μL of 4% formaldehyde-H_2 and 10 μL 4% formaldehyde-D_2, respectively [29,30] and mixed thoroughly. The mixtures were vortexed for 5 min, immediately followed by the addition of 10 μL of 0.6 M sodium cyanoborohydride and vortexed for 1 h at room temperature. The resultant liquids were acidified by 10% TFA/ H_2O to pH 2.0~3.0 and applied onto the in-house reverse phase C18 column pre-equilibrated with 200 μL of 0.1% TFA/H_2O (pH 2.0~3.0) for desalting. The column was also washed with 200 μL of 0.1% TFA/H_2O (pH 3.0) and then eluted with a stepwise ACN gradient from 50% to 100% in 0.1% TFA at room temperature.

Hydrophilic interaction chromatography (HILIC) for peptide separation

HILIC was performed on an L-7100 pump system with quaternary gradient capability (Hitachi, Tokyo, Japan) using a TSK gel Amide-80 HILIC column (2.0×150 mm, 3 μm; Tosoh Biosciences, Tokyo, Japan) [31-33] with a flow rate of 200 μL/min. Two buffers were used for gradient elution: solvent (A), 0.1% TFA in water, and solvent (B), 0.1% TFA in 100% ACN. The eluted fractions from the reverse-phase C18 column were each dissolved in 25 μL of solution containing 85% ACN and 0.1% TFA and then injected into the 20 μL sample loop. The gradient was processed as follows: 98% (B) for 5 min, 98-85% (B) for 5 min, 85-0% (B) for 40 min, 0% (B) for 5 min, 0-98% (B) for 2 min and 98% (B) for 3 min. A total of 10 fractions were collected (1.2 mL for each fraction) and dried in a vacuum centrifuge.

Nano LC-MS/MS analysis

The lyophilized powders were reconstituted in 10 μL of 0.1% FA in H_2O and analyzed by LTQ Orbitrap XL (Thermo Fisher Scientific, San Jose, CA). Reverse phase nano-LC separation was performed on an Agilent 1200 series nano-flow system (Agilent Technologies, Santa Clara, CA). A total of 10 μL sample from collected fractions was loaded onto an Agilent Zorbax XDB C18 precolumn (0.35 mm, 5 μm), followed by separation using an in-house C18 column (i.d. 75 μm×15 cm, 3 μm). The mobile phases used were (A) 0.1% FA in water and (B) 0.1% FA in 100% ACN. A linear gradient from 5% to 95% of (B) over a 70-min period at a flow rate of 300 nL/min was applied. The peptides were analyzed in the positive ion mode by applying a voltage of 1.8 kV to the injection needle. The MS was operated in a data-dependent mode, in which one full scan was used with m/z 400-1600 in the Orbitrap at a scan rate of 30 ms/scan. The fragmentation was performed using the CID mode with collision energy of 35 V. A repeat duration of 30 s was applied to exclude the same m/z ions from

the reselection for fragmentation. Xcalibur software (version 2.0.7, Thermo Fisher Scientific, San Jose, CA) was used for the management of instrument control, data acquisition, and data processing.

Protein database search and characterization

Peptides were identified by peak lists converted from the nanoLC-MS/MS spectra by bioinformatics searching against *Homo sapiens* taxonomy in the Swiss-Prot databases for exact matches using the Mascot search program (http://www.matrixscience.com) [34,35]. Parameters were set as follows: a mass tolerance of 0.1 Da for precursor ions and 0.8 Da for fragment ions; no missed cleavage sites allowed for trypsin; carbamidomethyl cysteine specified as fixed modification; dimethylation specified as standard for the quantification; oxidized methionine and deamidated asparagine/glutamine as optional modification. Peptides were considered positively identified if their Mascot individual ion score was higher than 20 ($p<0.05$).

Subsequently, the analysis of peptide quantification ratio (D/H) for normal (hydrogen labeling) and RCC tissues (deuterium labeling) was carried out by Mascot Distiller program (version 2.3, Matrix Science Ltd., London, U.K.) using the average area of the first 3 isotopic peaks across the elution profile. The Mascot search data as well as quantification results from each fraction were also merged by this program that combined the peptide ratios matching the same sequence obtained from different fractions or at different retention time and charge states [30]. The identified proteins with up- and down-regulation were further categorized based on their biological process and molecular function using the PANTHER classification system (http://www.pantherdb.org) as described in the previous studies [36-38].

Construction of signaling pathways and network analysis of protein interaction

The software program (www.ingenuity.com) from Ingenuity Pathways Analysis (IPA, Ingenuity Systems, Redwood City, CA) was used for deriving the pathways and networks of protein interaction, and the involved prospective mechanism. Protein factors characterized by proteomic analysis were analyzed for their association with mapping related to canonical pathways deposited in the IPA library.

Results and Discussion

Analysis of protein expression levels by nanoLC-MS/MS

Quantitative proteome analysis by application of shotgun proteomics analysis coupled with stable isotope dimethyl labeling has been successfully used in examining candidate biomarkers or target factors in different types of cells due to the fact that this unique quantitative labeling approach can detect differentially expressed proteins at relatively low abundance [20,26,27,30]. In this study, we conducted a comparative proteomics analysis of RCC by shotgun proteomic approach. A schematic of sample processing, separation and the subsequent workflow concerning trypsin digestion, dimethyl labeling and shotgun analysis is presented in Figure 1. Initially, respective tryptic peptides with hydrogen and deuterium were mixed in a 1:1 (w/w) ratio and then enriched by the reverse-phase C_{18} column. Owing to the fact that the enriched peptide population was too complex to be fully detected and characterized by a single LC-MS/MS run, the enriched peptides were fractionated by HILIC based on polarity difference, and then harvested into 10 fractions. Each fraction was analyzed by LC-LTQ-Orbitrap and the parameter used for searching identified peptides was set to allow for no missed cleavage. Most of the peptides were separated from a single or two adjacent HILIC fractions, and peptides identified by Mascot search program (http://www.matrixscience.com) were accepted if their individual ion score was higher than 20, which had been a cutoff point used for the lower-quality MS/MS spectra [39-41].

Identification and quantification of differentially expressed proteins

All peptide sequences identified from three data sets were merged for identification and quantification. Once the differentially expressed proteins with confident identification based on dimethyl labeling, enzyme digestion and peptide mass fingerprinting were completed, the peptide quantification ratio (D/H) was then obtained by Mascot Distiller program using the average area of the first 3 isotopic peaks across each elution profile [28,30,42]. Herein, the 18 up-regulated (D/H ratio ≥ 2) and 48 down-regulated (D/H ratio ≤ 0.5) proteins displayed in at least three of five RCC tissues were identified and listed in Tables 1 and 2, respectively. The amino acid sequence coverage of the up-regulated proteins ranged from 22 to 68%. Many of these identified proteins in

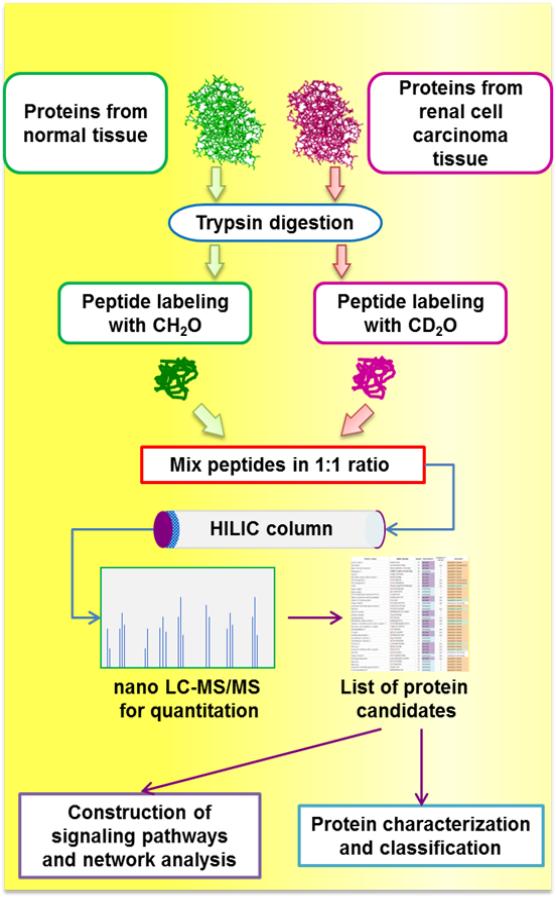

Figure 1: Experimental scheme of the procedures used for the screening of differentially expressed proteins. After lysis and enzymatic digestion, peptides were labeled with stable isotope and the differentially dimethyl-labeled products were then analyzed after desalting and fractionation. The quantitative shotgun analysis of proteome changes from clinical samples of renal clear cell carcinoma (RCC) and normal tissues was carried out by using HILIC-C18 peptide separation and nano LC-MS/MS coupled with stable isotope dimethyl labeling.

the expression profile have been previously reported in RCC, including down-regulation of serine hydroxymethyltransferase, betaine--homocysteine S-methyltransferase 1, glutamate dehydrogenase 1, delta-1-pyrroline-5-carboxylate dehydrogenase and aromatic-L-amino-acid decarboxylase involved in amino acid metabolism, fructose-bisphosphate aldolase B, fructose-1,6-bisphosphatase 1, and phosphoenolpyruvate carboxykinase involved in gluconeogenesis pathway.

In addition, the up-regulated proteins including cytochrome b5, ATP synthase subunit beta, electron transfer flavoprotein subunit beta and alpha involved in ATP generation, keratin type II cytoskeletal 8, vimentin, tropomyosin alpha-1 chain and annexin family were also detected in shotgun approach and reported previously [20,30,43,44], signifying that this up- or down-regulated effect may be universal among patients. On top of these known proteins, several novel changes in differentially expressed proteins were found, including down-regulation of calbindin, glycine amidinotransferase, guanine deaminase, L-xylulose reductase, transthyretin, ribonuclease UK114, vitamin D-binding protein, Xaa-Pro dipeptidase, Na(+)/H(+) exchange regulatory cofactor NHE-RF1, bifunctional ATP-dependent dihydroxyacetone kinase/FAD-AMP lyase and up-regulation of 39S ribosomal protein L43 (MRPL43). Figure 2 showed the peaks for representative peptides, including glycine amidinotransferase and ribonuclease UK114 as mentioned above. The isotopic pairs of nano-LC and MS/MS CID spectra shown in Figure 2A revealed that D_4- and H_4-labeled peptides (TPDFESTGLYSAMPR) derived from glycine amidinotransferase had m/z values of 850.41 (+2) and 852.41 (+2), respectively, and a D/H ratio of 0.12, were eluted simultaneously (~16 min) in the HILIC fraction 5. Figure 2B showed that the isotopic pairs (quantification ratios) of nano-LC and MS/MS CID spectra of D_4- and H_4-labeled peptides (TTVLLADINDFNTVNEIYK) from ribonuclease UK114, which had m/z values of 1120.10 (+2) and 1124.13 (+2) respectively, and a D/H ratio of 0.03, were eluted simultaneously (~20 min) in HILIC fraction 5. The above results further confirmed the absence of an isotopic effect in the two-dimensional HILIC-C18 separation and excellent efficiency in separating dimethylated peptides fractionated by HILIC column. We hypothesize that the improved efficiency resulted mainly from the high orthogonality of HILIC and the reverse-phase C_{18} column.

All these differentially expressed proteins between RCC and normal tissues were further categorized using the PANTHER classification system. Functional distributions of these identified proteins were shown in Figure 3. It is worth noting that binding and structural proteins accounted for 43% and 33% of up-regulated proteins, respectively (Figure 3A) and catalytic enzymes occupied as high as 73% of down-regulated proteins (Figure 3B). These identified proteins were also associated with a variety of biological processes such as cellular process (21%), transport (9%), metabolic process (14%), and cell communication (10%) as shown in Figure 4A; a high proportion of down-regulated proteins involved in metabolism (59%), metabolites and energy (12%) were shown in Figure 4B. However, it is unexpected to find that many proteins of alterations, which include over-expression of periostin, basement membrane-specific heparan sulfate proteoglycan core protein, 2-oxoglutarate dehydrogenase, protein S100-A9, plastin-2, etc. or under-expression of cofilin-1, agmatinase, 60S acidic ribosomal protein P2, ras-related protein Rab-14, glutaredoxin-1, etc. were not universal among all the matched tissue pairs and shown only in one or two individual RCC samples in our study. For some patients, several identified proteins including cathepsin D, peptidyl-prolyl cis-trans isomerase A, heterogeneous nuclear ribonucleoproteins A2/B1, etc. in RCC tissues were shown to be anomalously lower, equal or higher than those in their matched normal tissues. The rudimentary reasons for these variations are not clear. It appears that a large number of matched sample pairs should be acquired in order to discriminate the subtle but crucial differences between RCC and corresponding normal tissues. This can certainly clarify whether these identified proteins with anomalous results are involved in the carcinogenesis.

Protein ID	Fold change	p-value	Number of sample pairs	Gene symbol	Swiss-Prot accession number	pI / mass (kDa)	Score / match	Sequence coverage %
39S ribosomal protein L43, mitochondrial	134.8~246.1	0.0269	3 / 5	MRPL43	Q8N983	8.97 / 23.8	619 / 400	22
Histone H4	10.5~22.9	0.0479	3 / 5	HIST1H4A	P62805	11.36 / 11.7	213 / 22	38
Annexin A1	2.6~13.9	0.0997	4 / 5	ANXA1	P04083	6.57 / 39.9	560 / 47	39
Annexin A2	5.4~13.2	0.1362	3 / 5	ANXA2	P07355	7.57 / 39.8	785 / 63	55
Keratin, type II cytoskeletal 8	5.2~10.3	0.0978	3 / 5	KRT8	P05787	5.52 / 54.7	891 / 60	51
Histone H2A type 2-A	2.1~10.2	0.2082	3 / 5	H2A2A	Q6FI13	10.90 / 14.1	689 / 36	49
Vimentin	3.7~6.8	0.0209	4 / 5	VIM	P08670	5.06 / 54.3	11182 / 601	53
Filamin-A	2.6~6.5	0.0706	3 / 5	FLNA	P21333	5.70 / 288.4	425 / 165	32
Keratin, type I cytoskeletal 18	4.4~6.3	0.0822	3 / 5	KRT18	P05783	5.34 / 48.7	1394 / 89	53
Tropomyosin alpha-1 chain	2.1~6.1	0.0443	4 / 5	TPM1	P09493	4.69 / 34.0	87 / 46	38
Pyruvate kinase isozymes M1/M2	2.5~5.6	0.0220	4 / 5	PKM2	P14618	7.96 / 59.7	3712 / 142	48
Ras GTPase-activating-like protein IQGAP1	2.6~5.3	0.1445	4 / 5	IQGAP1	P46940	6.08 / 194.1	456/106	27
Galectin-1	3.3~5.3	0.0874	3 / 5	LGALS1	P09382	5.34 / 15.3	82 / 13	68
Carbonic anhydrase 1	2.3~3.8	0.1208	3 / 5	CA1	P00915	6.59 / 29.5	351 / 26	40
Transgelin	2.1~3.0	0.0047	4 / 5	TAGLN	Q01995	8.87 / 23.2	815/112	54
L-lactate dehydrogenase A chain	2.2~2.8	0.2245	3 / 5	LDHA	P00338	8.44 / 37.8	459 / 22	38
Annexin A4	2.5~2.8	0.0490	3 / 5	ANXA4	P09525	5.84 / 36.2	953 / 25	35
Clathrin heavy chain 1	2.0~2.8	0.1907	3 / 5	CLTC	Q00610	5.48 / 196.3	994 / 114	30

D = Deuterium labeling (RCC tissues); H = Hydrogen labeling (normal tissues)

Table 1: Up-regulated proteins (D/H ratio ≥ 2) were displayed in at least three of five renal clear cell carcinoma (RCC) tissues analyzed by nano LC-MS/MS coupled with stable isotope dimethyl labeling.

Protein ID	Fold change	p-value	Number of sample pairs	Gene symbol	Swiss-Prot accession number	pI / mass (kDa)	Score / match	Sequence coverage %
Enoyl-CoA hydratase, mitochondrial	15.8~23.1	<0.001*	5 / 5	ECHS1	P30084	8.34 / 32.5	1267 / 51	37
Phosphoenolpyruvatecarboxykinase [GTP], mitochondrial	13.5~60.0	<0.001*	5 / 5	PCK2	Q16822	7.57 / 72.1	53 / 28	23
Argininosuccinate synthase	13.3~37.7	0.409	3 / 5	ASS1	P00966	8.08 / 47.8	664 / 35	54
Delta-1-pyrroline-5-carboxylate dehydrogenase, mitochondrial	9.9~17.5	<0.001*	5 / 5	ALDH4A1	P30038	8.25 / 63.1	2221 / 100	27
Methylmalonate-semialdehyde dehydrogenase [acylating], mitochondrial	8.7~27.7	0.854	3 / 5	ALDH6A1	Q02252	8.72 / 59.2	485 / 44	51
Glycine amidinotransferase, mitochondrial	8.3~24.5	<0.001*	5 / 5	GATM	P50440	8. 26 / 49.6	415 / 33	39
Bifunctional ATP-dependent dihydroxyacetone kinase/FAD-AMP lyase (cyclizing)	7.7~18.4	0.347	3 / 5	DAK	Q3LXA3	7.12 / 59.2	188 / 28	38
Ribonuclease UK114	6.9~29.1	0.001	3 / 5	HRSP12	P52758	8.74 / 14.8	156 / 14	37
Dihydropyrimidinase	6.6~38.4	0.002	3 / 5	DPYS	Q14117	6.81 / 58.1	505 / 19	27
Betaine--homocysteine S-methyltransferase 1	6.2~18.2	0.963	4 / 5	BHMT	Q93088	6.58 / 46.3	892 / 39	38
Calbindin	6.0~48.6	0.005	4 / 5	CALB1	P05937	4.70 / 31.0	158 / 13	29
Fructose-bisphosphatealdolase B	5.3~25.3	<0.001*	5 / 5	ALDOB	P05062	8.00 / 40.6	1592 / 160	73
Aromatic-L-amino-acid decarboxylase	4.9~21.9	<0.001*	4 / 5	DDC	P20711	6.77 / 55.2	68 / 15	19
3-ketoacyl-CoA thiolase, mitochondrial	4.8~6.3	0.514	3 / 5	ACAA2	P42765	8.32 / 43.1	191 / 35	41
Ketohexokinase	4.6~26.6	0.299	4 / 5	KHK	P50053	5.64 / 33.5	622 / 111	21
Aminoacylase-1	4.3~30.8	<0.001*	4 / 5	ACY1	Q03154	5.77 / 46.5	102 / 23	43
Xaa-Pro dipeptidase	4.3~23.7	0.006	3 / 5	PEPD	P12955	5.64 / 55.8	151 / 24	28
L-xylulosereductase	4.1~12.3	<0.001*	4 / 5	DCXR	Q7Z4W1	8.33 / 26.4	635 / 23	36
Hydroxymethylglutaryl-CoA lyase, mitochondrial	4.0~5.7	0.596	3 / 5	HMGCL	P35914	8.81 / 35.4	142 / 48	28
Mu-crystallin homolog	3.8~23.7	<0.001*	4 / 5	CRYM	Q14894	5.06 / 34.4	437 / 14	40
3-ketoacyl-CoA thiolase, peroxisomal	3.6~22.7	0.883	3 / 5	ACAA1	P09110	8.76 / 45.4	874 / 35	49
Vitamin D-binding protein	3.4~4.9	0.028	3 / 5	GC	P02774	5.40 / 54.5	145 / 14	17
Glutathione S-transferase A1	3.3~50.6	<0.001*	5 / 5	GSTA1	P08263	8.91 / 26.3	802 / 84	67
Medium-chain specific acyl-CoA dehydrogenase, mitochondrial	3.2~9.6	<0.001*	4 / 5	ACADM	P11310	8.61 / 47.8	130 / 13	31
Sodium/potassium-transporting ATPase subunit alpha-1	3.2~7.6	0.567	3 / 5	ATP1A1	P05023	5.33 / 115.9	575 / 50	19
Aconitatehydratase, mitochondrial	2.5~35.0	0.003	4 / 5	ACO2	Q99798	7.36 / 87.7	313 / 49	27
Fructose-1,6-bisphosphatase 1	3.0~29.6	0.738	3 / 5	FBP1	P09467	6.54 / 38.0	469 / 26	36
Transthyretin	5.4~9.4	<0.001*	4 / 5	TTR	P02766	5.52 / 16.2	610 / 54	49
Serine hydroxymethyltransferase, cytosolic	3.2~4.8	0.389	3 / 5	SHMT1	P34896	7.61 / 54.5	191 / 40	35
Na(+)/H(+) exchange regulatory cofactor NHE-RF1	3.6~10.7	0.221	3 / 5	SLC9A3R1	O14745	5.55 / 39.1	92 / 23	36
Glutamate dehydrogenase 1, mitochondrial	3.0~5.3	0.065	3 / 5	GLUD1	P00367	7.66 / 62.6	60 / 24	34
Succinyl-CoA ligase [GDP-forming] subunit beta, mitochondrial	2.6~15.6	0.246	3 / 5	SUCLG2	Q96I99	6.15 / 47.8	116 / 26	34
Hydroxyacyl-coenzyme A dehydrogenase, mitochondrial	2.6~5.4	<0.001*	5 / 5	HADH	Q16836	8.88 / 35.2	1089 / 45	48
Complement C3	2.5~3.1	0.737	3 / 5	C3	P01024	6.02 / 192.2	2313 / 172	40
Alpha-crystallin B chain	2.7~4.1	0.560	3 / 5	CRYAB	P02511	6.76 / 20.4	4522 / 602	72
Acetyl-CoA acetyltransferase, mitochondrial	2.4~4.0	0.946	3 / 5	ACAT1	P24752	8.98 / 46.4	670 / 64	55
Carbonic anhydrase 2	2.4~74.2	0.889	3 / 5	CA2	P00918	6.87 / 30.0	229 / 51	34
60 kDa heat shock protein, mitochondrial	2.4~5.5	0.073	3 / 5	HSPD1	P10809	5.70 / 62.7	12507/ 660	65
Delta(3,5)-Delta(2,4)-dienoyl-CoA isomerase, mitochondrial	2.3~4.9	<0.001*	4 / 5	ECH1	Q13011	8.16 / 36.68	279 / 13	35
Cytochrome b5	2.3~9.9	0.637	3 / 5	CYB5A	P00167	4.88 / 15.5	392 / 21	55
ATP synthase subunit beta, mitochondrial	2.3~3.3	0.169	3 / 5	ATP5B	P06576	5.26 / 57.2	1348 / 130	63
Guanine deaminase	2.2~5.3	0.659	3 / 5	GDA	Q9Y2T3	5.44 / 51.4	47 / 24	35
Thioredoxin-dependent peroxide reductase, mitochondrial	2.3~6.3	0.996	3 / 5	PRDX3	P30048	7.67 / 28.4	256 / 21	42
Quinone oxidoreductase	2.1~7.7	<0.001*	5 / 5	CRYZ	Q08257	8.56 / 36.0	495 / 36	41
UDP-glucuronosyltransferase 2B7	2~14.0	0.426	3 / 5	UGT2B7	P16662	8.54 / 62.2	77 / 22	33
Electron transfer flavoprotein subunit beta	2.0~4.4	0.015	3 / 5	ETFB	P38117	8.24 / 28.8	34 / 21	30
Electron transfer flavoprotein subunit alpha, mitochondrial	2.2~10.4	0.020	3 / 5	ETFA	P13804	8.62 / 115.9	1110 / 50	45
L-lactate dehydrogenase B chain	2.1~8.7	0.006	3 / 5	LDHB	P07195	5.71 / 37.6	672 / 68	63

D = Deuterium labeling (RCC tissues); H = Hydrogen labeling (normal tissues)
Statistically significant data by student *t*-test

Table 2: Down-regulated proteins (D/H ratio ≤ 0.5) were displayed in at least three of five renal clear cell carcinoma (RCC) tissues analyzed by nanoLC-MS/MS coupled with stable isotope dimethyl labeling.

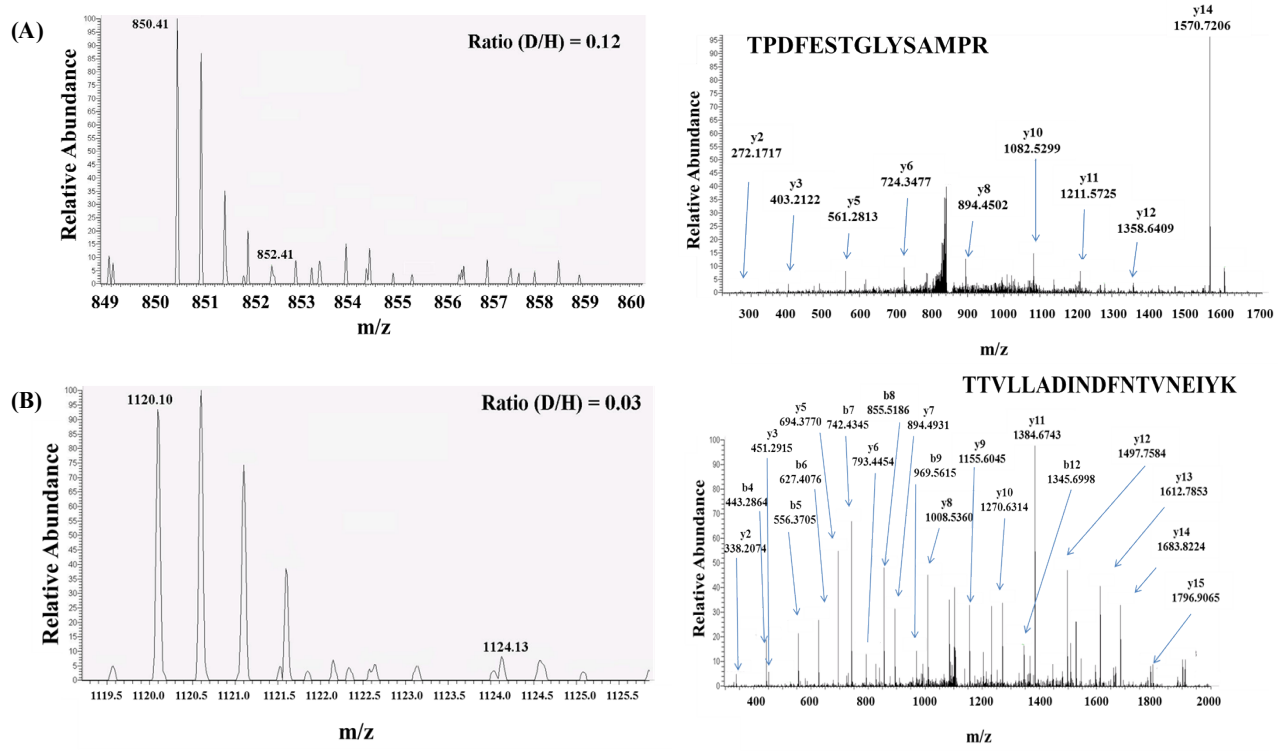

Figure 2: The MS/MS CID spectra and ratios of isotopic pairs (quantification ratios) of the representative peptides TPDFESTGLYSAMPR for glycine amidinotransferase (A) and TTVLLADINDFNTVNEIYK for ribonuclease UK114 (B). Peptide quantification ratios (D/H) for RCC (deuterium labeling) and normal (hydrogen labeling) were calculated by Mascot Distiller program using the average area of the first three isotopic peaks across the elution profile. The program merged the Mascot search data and quantification results from each fraction, and peptide ratios for the same sequences obtained from different fractions or at different retention times and charge states were combined for further analysis.

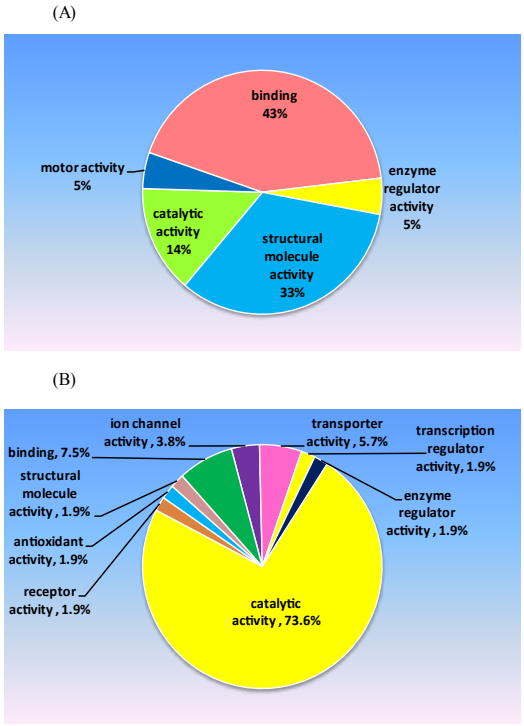

Figure 3: Molecular function distribution of up- (A) and down-regulated (B) proteins identified by nanoLC-MS/MS in renal clear cell carcinoma (RCC) tissue.

RCC-associated proteins

It has been suggested that ribosomal proteins together with other related members are involved in promoting the interaction of ribosomes with the mitochondrial inner membrane and also in the synthesis of hydrophobic proteins. These hydrophobic proteins, components of the enzyme complexes in oxidative phosphorylation system, are responsible for about 90% ATP generation in eukaryotic organisms [45]. Interestingly, our study demonstrates that ATP generation components of mitochondrial proteins including cytochrome b5, ATP synthase subunit beta, electron transfer flavoprotein subunit beta and alpha were down-regulated. In addition, mitochondrial glycine amidinotransferase with D/H ratio ranging from 0.04 to 0.12 also showed 8.3 to 24.5 fold down-regulation in all five RCC tissues (Table 2). This enzyme is responsible for catalyzing the committed step in the formation of creatine, which will facilitate to buffer the rapid changes in ADP/ATP ratio in tissues [46,47]. The previous study [20] of another group also showed the down-regulation of ubiquinol cytochrome c reductase (UQCR) as well as NADH-ubiquinone oxidoreductase complex I in RCC. Based on these data, RCC can be characterized partially as a result of the dysfunction of energy buffering and altered energy metabolism. These results highlighted by a series of down-regulated proteins suggest that the clear-cut decrease of ATP generation components related to mitochondrial dysfunction appears to be involved in RCC carcinogenesis.

Furthermore, ribonuclease UK114, responsible for blocking translation by cleaving phosphodiester bonds only in single-stranded RNA, is an endoribonuclease predominantly present in human adult kidney and liver [48]. It has been reported that protein expression levels are remarkably reduced in hepatocellular tumors compared with normal liver tissues. This result gave rise to the suggestion that ribonuclease UK114 may be an important biomarker for hepatic carcinoma [49]. Therefore, our current observation demonstrates that the reduced expression of ribonuclease UK114 in RCC raises the possibility of its association and correlation with the pathologic status and carcinogenesis of RCC formation..

Construction of RCC signaling pathways and network based on bioinformatics

Theoretically, most of the related or disease-oriented factors, once quite a few or enough ones identified, may be clustered and classified into a specific pathway dominating the maintenance and progression of carcinogenic state. By a panel of these identified proteins, we can further construct the expected feasible pathways to account for the biochemical characterization related to RCC. In Figure 5, these identified proteins mapped to canonical pathways from the Ingenuity Pathways Analysis (IPA, Ingenuity Systems) library were shown in green color to indicate the up-regulation and red color to indicate the down-regulation, and also displayed with different shapes to indicate the different functions. All the gray arrows indicate the biological interrelationships between these molecules. All arrows in the figure were supported by at least one reference from the literature, textbooks, or canonical information stored in the Ingenuity Knowledge Base. As shown in Figure 5A, up-regulated proteins including ANXA2, LGALS1, VIM and TPM1, to some extent, are involved in metastasis, angiogenesis, tumor invasion and growth; simultaneously, down-regulated ones including CRYAB, GSTA1, CALB1 and HSPD1 were categorized to apoptosis (Figure 5B). Namely, RCC was characterized not with a single enzymatic or cytoskeletal alteration but with a series of characteristic and functional changes.

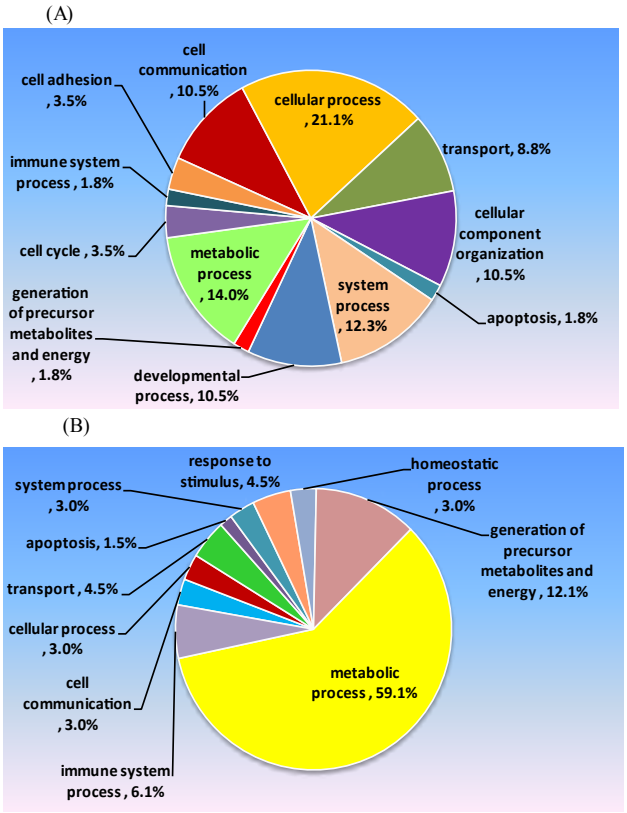

Figure 4: Biological process of up- (A) and down-regulated (B) proteins identified by nanoLC-MS/MS in renal clear cell carcinoma (RCC) tissue.

In this result, several novel proteins identified by our shotgun approach were not mapped to the canonical pathway constructed in the database due to the fact that these proteins were not linked to functional interaction; however, the importance of these unmapped proteins with universal down-regulation cannot be overlooked and the potential of these proteins serving as candidate biomarkers will be validated by subjecting them into verification and validation using ion scanning of peptides measured and quantified in multiple reaction monitoring (MRM) mode of nano LC-MS/MS. Therefore, this proteomics approach demonstrates a prospective potential application to monitoring the expression level of a large number of cellular proteins and further offering more candidate proteins complementary to previously identified targets in the literature.

In conclusion, instead of one universal tumorigenesis enzyme being detected for some specific types of cancer, RCC involves a variety of protein factors including ANXA2, LGALS1, VIM and TPM1 related to metastasis, angiogenesis, tumor invasion and tumor growth, in addition to CRYAB, [50] GSTA1, CALB1 and HSPD1, which are linked to apoptosis function. Moreover, the clear-cut decrease of ATP generation components related to mitochondrial dysfunction appears to be also involved in RCC carcinogenesis. The systematic decrease or increase of these enzymes related to altered energy metabolism may be responsible for the dysfunction of kidney cells, followed by morphological aberrations upon progressive developments of RCC. Prospectively, the proteomic analysis carried out in this pilot project should be extended to form a solid basis for the development of a

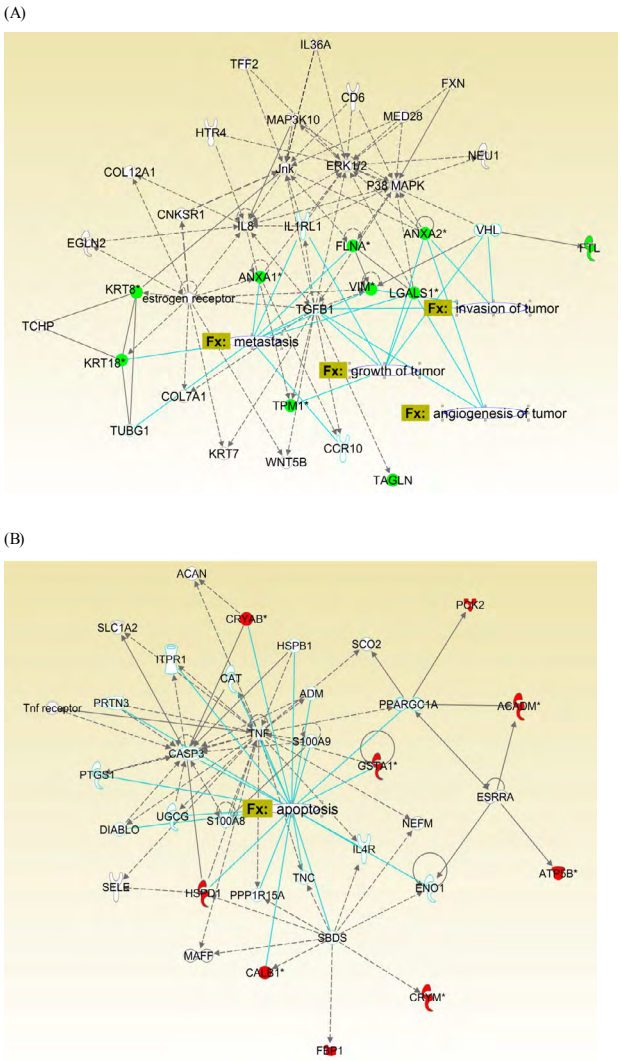

Figure 5: Schematic representation of derived pathways associated with renal clear cell carcinoma. The networks of these identified proteins mapped to canonical pathways from the Ingenuity Pathways Analysis (IPA, Ingenuity Systems) library were used to compare up-regulated (A) or down-regulated (B) protein molecules between normal and diseased tissues. Identified proteins with up- and down-regulation are displayed in green and red, respectively and have different shapes to indicate different functions associated with metastasis, tumor growth, invasion and angiogenesis. The gray arrows indicate the biological interrelationships between molecules.

specific and high-throughput protocol based on multiple reaction monitoring (MRM) in order to verify and validate the potential biomarkers detected and identified from both RCC patients and healthy controls in the future. In the near future, our comparative proteome data from urine samples may not only offer a novel approach to further understand RCC metabolism in relation to its underlying mechanism of carcinogenesis, but also develop potential biomarker candidates for the non-invasive diagnosis and prognosis (Supplementary Data 1 and 2).

Acknowledgements

This work was supported in part by Kaohsiung Medical University (KMU), Academia Sinica and the National Science Council (NSC Grants 100-2320-B-037-019, 101-2113-M-037-004 and 102-2320-B-037-025 to S.-H. Chiou), Taipei, Taiwan. We thank the core facility grant support (NSC Grant 99-2745-B-037-005 to S.H. Chiou) at the Center for Research Resources and Development (CRRD), Kaohsiung Medical University under the auspices of National Science Council. We also thank Edward Hsi, Department of Medical Research, Kaohsiung Medical University Hospital for his kind assistance in data analysis.

Conflict of Interest

The authors have declared no conflict of interest.

References

1. Lam JS, Leppert JT, Belldegrun AS, Figlin RA (2005) Novel approaches in the therapy of metastatic renal cell carcinoma. World J Urol 23: 202-212.
2. Mickisch GH, Mattes RH (2005) Combination of surgery and immunotherapy in metastatic renal cell carcinoma. World J Urol 23: 191-195.
3. Yuan JM, Castelao JE, Gago-Dominguez M, Ross RK, Yu MC (1998) Hypertension, obesity and their medications in relation to renal cell carcinoma. Br J Cancer 77: 1508-1513.
4. Ljungberg B, Campbell SC, Choi HY, Jacqmin D, Lee JE, et al. (2011) The epidemiology of renal cell carcinoma. EurUrol 60: 615-621.
5. Murai M, Oya M (2004) Renal cell carcinoma: etiology, incidence and epidemiology. CurrOpinUrol 14: 229-233.
6. Ahn YS, Zerban H, Bannasch P (1993) Expression of glucose transporter isoforms (GLUT1, GLUT2) and activities of hexokinase, pyruvate kinase, and malic enzyme in preneoplastic and neoplastic rat renal basophilic cell lesions. Virchows Arch B CellPatholInclMolPathol 63: 351-357.
7. Steinberg P, Störkel S, Oesch F, Thoenes W (1992) Carbohydrate metabolism in human renal clear cell carcinomas. Lab Invest 67: 506-511.
8. Uzzo RG, Rayman P, Kolenko V, Clark PE, Cathcart MK, et al. (1999) Renal cell carcinoma-derived gangliosides suppress nuclear factor-kappaB activation in T cells. J Clin Invest 104: 769-776.
9. Castilla EA, Liou LS, Abrahams NA, Fergany A, Rybicki LA, et al. (2002) Prognostic importance of resection margin width after nephron-sparing surgery for renal cell carcinoma. Urology 60: 993-997.
10. Fergany AF, Hafez KS, Novick AC (2000) Long-term results of nephron sparing surgery for localized renal cell carcinoma: 10-year followup. J Urol 163: 442-445.
11. Wettersten HI, Weiss RH (2013) Potential biofluid markers and treatment targets for renal cell carcinoma. Nat Rev Urol 10: 336-344.
12. Rini BI, Rathmell WK, Godley P (2008) Renal cell carcinoma. CurrOpinOncol 20: 300-306.
13. Thoenes W, Störkel S, Rumpelt HJ (1986) Histopathology and classification of renal cell tumors (adenomas, oncocytomas and carcinomas). The basic cytological and histopathological elements and their use for diagnostics. Pathol Res Pract 181: 125-143.
14. Ulrich W, Buxbaum P, Holzner JH (1988) Pathology of renal cancer and its metastases. SeminSurgOncol 4: 143-148.
15. Delahunt B, Eble JN, McCredie MR, Bethwaite PB, Stewart JH, et al. (2001) Morphologic typing of papillary renal cell carcinoma: comparison of growth kinetics and patient survival in 66 cases. Hum Pathol 32: 590-595.
16. Sika-Paotonu D, Bethwaite PB, McCredie MR, William Jordan T, Delahunt B (2006) Nucleolar grade but not Fuhrman grade is applicable to papillary renal cell carcinoma. Am J SurgPathol 30: 1091-1096.
17. Delahunt B, Sika-Paotonu D, Bethwaite PB, William Jordan T, Magi-Galluzzi C, et al. (2011) Grading of clear cell renal cell carcinoma should be based on nucleolar prominence. Am J SurgPathol 35: 1134-1139.
18. Bukowski RM, Rayman P, Uzzo R, Bloom T, Sandstrom K, et al. (1998) Signal transduction abnormalities in T lymphocytes from patients with advanced renal carcinoma: clinical relevance and effects of cytokine therapy. Clin Cancer Res 4: 2337-2347.
19. Chiou SH, Wu CY (2011) Clinical proteomics: current status, challenges, and future perspectives. Kaohsiung J Med Sci 27: 1-14.
20. Unwin RD, Craven RA, Harnden P, Hanrahan S, Totty N, et al. (2003) Proteomic changes in renal cancer and co-ordinate demonstration of both the glycolytic and mitochondrial aspects of the Warburg effect. Proteomics 3: 1620-1632.

21. Ideker T, Thorsson V, Ranish JA, Christmas R, Buhler J, et al. (2001) Integrated genomic and proteomic analyses of a systematically perturbed metabolic network. Science 292: 929-934.

22. Shi T, Dong F, Liou LS, Duan ZH, Novick AC, et al. (2004) Differential protein profiling in renal-cell carcinoma. MolCarcinog 40: 47-61.

23. Sarto C, Marocchi A, Sanchez JC, Giannone D, Frutiger S, et al. (1997) Renal cell carcinoma and normal kidney protein expression. Electrophoresis 18: 599-604.

24. Lichtenfels R, Kellner R, Atkins D, Bukur J, Ackermann A, et al. (2003) Identification of metabolic enzymes in renal cell carcinoma utilizing PROTEOMEX analyses. BiochimBiophysActa 1646: 21-31.

25. Seliger B, Dressler SP, Lichtenfels R, Kellner R (2007) Candidate biomarkers in renal cell carcinoma. Proteomics 7: 4601-4612.

26. Huang SY, Tsai ML, Wu CJ, Hsu JL, Ho SH, et al. (2006) Quantitation of protein phosphorylation in pregnant rat uteri using stable isotope dimethyl labeling coupled with IMAC. Proteomics 6: 1722-1734.

27. Wu CJ, Hsu JL, Huang SY, Chen SH (2010) Mapping N-terminus phosphorylation sites and quantitation by stable isotope dimethyl labeling. J Am Soc Mass Spectrom 21: 460-471.

28. Santos HM, Kouvonen P, Capelo JL, Corthals GL (2012) Isotopic labelling of peptides in tissues enhances mass spectrometric profiling. Rapid Commun Mass Spectrom 26: 254-262.

29. Boersema PJ, Aye TT, van Veen TA, Heck AJ, Mohammed S (2008) Triplex protein quantification based on stable isotope labeling by peptide dimethylation applied to cell and tissue lysates. Proteomics 8: 4624-4632.

30. Craven RA, Stanley AJ, Hanrahan S, Dods J, Unwin R, et al. (2006) Proteomic analysis of primary cell lines identifies protein changes present in renal cell carcinoma. Proteomics 6: 2853-2864.

31. Yoshida T (1997) Peptide separation in normal phase liquid chromatography. Anal Chem 69: 3038-3043.

32. Yoshida T (1998) Calculation of peptide retention coefficients in normal-phase liquid chromatography. J Chromatogr A 808: 105-112.

33. Alpert AJ (1990) Hydrophilic-interaction chromatography for the separation of peptides, nucleic acids and other polar compounds. J Chromatogr 499: 177-196.

34. Perkins DN, Pappin DJ, Creasy DM, Cottrell JS (1999) Probability-based protein identification by searching sequence databases using mass spectrometry data. Electrophoresis 20: 3551-3567.

35. Hirosawa M, Hoshida M, Ishikawa M, Toya T (1993) MASCOT: multiple alignment system for protein sequences based on three-way dynamic programming. ComputApplBiosci 9: 161-167.

36. Mi H, Muruganujan A, Thomas PD (2013) PANTHER in 2013: modeling the evolution of gene function, and other gene attributes, in the context of phylogenetic trees. Nucleic Acids Res 41: D377-386.

37. Nikolsky Y, Bryant J (2009) Protein networks and pathway analysis. Preface. Methods MolBiol 563: v-vii.

38. Thomas PD, Kejariwal A, Guo N, Mi H, Campbell MJ, et al. (2006) Applications for protein sequence-function evolution data: mRNA/protein expression analysis and coding SNP scoring tools. Nucleic Acids Res 34: W645-650.

39. Thingholm TE, Jensen ON, Robinson PJ, Larsen MR (2008) SIMAC (sequential elution from IMAC), a phosphoproteomics strategy for the rapid separation of monophosphorylated from multiply phosphorylated peptides. Mol Cell Proteomics 7: 661-671.

40. Hou W, Ethier M, Smith JC, Sheng Y, Figeys D (2007) Multiplexed proteomic reactor for the processing of proteomic samples. Anal Chem 79: 39-44.

41. Pichler P, Köcher T, Holzmann J, Mazanek M, Taus T, et al. (2010) Peptide labeling with isobaric tags yields higher identification rates using iTRAQ 4-plex compared to TMT 6-plex and iTRAQ 8-plex on LTQ Orbitrap. Anal Chem 82: 6549-6558.

42. Webster J, Oxley D (2012) Protein identification by MALDI-TOF mass spectrometry. Methods MolBiol 800: 227-240.

43. Zimmermann U, Balabanov S, Giebel J, Teller S, Junker H, et al. (2004) Increased expression and altered location of annexin IV in renal clear cell carcinoma: a possible role in tumour dissemination. Cancer Lett 209: 111-118.

44. Kellner R, Lichtenfels R, Atkins D, Bukur J, Ackermann A, et al. (2002) Targeting of tumor associated antigens in renal cell carcinoma using proteome-based analysis and their clinical significance. Proteomics 2: 1743-1751.

45. Liu M, Spremulli L (2000) Interaction of mammalian mitochondrial ribosomes with the inner membrane. J BiolChem 275: 29400-29406.

46. Walker JB (1979) Creatine: biosynthesis, regulation, and function. AdvEnzymolRelat Areas MolBiol 50: 177-242.

47. Van Pilsum JF, Stephens GC, Taylor D (1972) Distribution of creatine, guanidinoacetate and the enzymes for their biosynthesis in the animal kingdom. Implications for phylogeny. Biochem J 126: 325-345.

48. Oka T, Tsuji H, Noda C, Sakai K, Hong YM, et al. (1995) Isolation and characterization of a novel perchloric acid-soluble protein inhibiting cell-free protein synthesis. J BiolChem 270: 30060-30067.

49. Chong CL, Huang SF, Hu CP, Chen YL, Chou HY, et al. (2008) Decreased expression of UK114 is related to the differentiation status of human hepatocellular carcinoma. Cancer Epidemiol Biomarkers Prev 17: 535-542.

50. Ho PY, Chueh SC, Chiou SH, Wang SM, Lin WC, et al. (2013) AlphaB-crystallin in clear cell renal cell carcinoma: tumor progression and prognostic significance. Urol Oncol 31: 1367-1377.

This article was originally published in a special issue, **Affinity Proteomics** handled by Editor(s). Dr. Peter Nilsson, KTH-Royal Institute of Technology, Sweden